Propionibacterium freudenreichii CIRM-BIA 129 mitigates colitis through S layer protein B-dependent epithelial strengthening. P. freudenreichii inhibits inflammation-induced epithelial break-down

Marine Mantel, Tony Durand, Anne Bessard, Ségolène Pernet, Julie Beaudeau, Juliana Guimaraes-Laguna, Marie-Bernadette Maillard, Eric Guédon, Michel Neunlist, Yves Le Loir, et al.

Propionibacterium freudenreichii CIRM-BIA 129 mitigates colitis through S layer protein B-dependent epithelial strengthening.

P. freudenreichii inhibits inflammation-induced epithelial break-down.

Marine Mantel[1, 2], Tony Durand[1], Anne Bessard[1], Ségolène Pernet[1], Julie Beaudeau[1,3], Juliana Guimaraes-Laguna[2], Marie-Bernadette Maillard[2], Eric Guédon[2], Michel Neunlist[1], Yves Le Loir[2], Gwénaël Jan[†2] and Malvyne Rolli-Derkinderen*[†1]

Affiliations:
1. nantes université, inserm, the enteric nervous system in gut and brain disorders, imad, f-44000 nantes, france
2. inrae, umr 1253, stlo, l'institut agro, f-35000 rennes, france
3. CRNH-OUEST
[†] these authors shared senior authorship
Corresponding author: malvyne.rolli-derkinderen@univ-nantes.fr

ABSTRACT

The growing incidence of human diseases involving inflammation and increased gut permeability makes the quest for protective functional foods more crucial than ever. *Propionibacterium freudenreichii (P. freudenreichii)* is a beneficial bacterium used in the dairy and probiotic industries. Selected strains exert anti-inflammatory effects, and the present work addresses whether the *P. freudenreichii* CIRM-BIA129, consumed daily in a preventive way, could protect mice from acute colitis induced by dextran sodium sulfate (DSS), and more precisely whether it could protect from intestinal epithelial breakdown induced by inflammation.

P. freudenreichii CIRM-BIA129 mitigated colitis severity and inhibited DSS-induced permeability. It limited crypt length reduction and promoted the expression of Zonula Occludens-1 (ZO-1), without reducing *interleukin-1beta* mRNA (*il-1ß*) expression. *In vitro*, *P. freudenreichii* CIRM-BIA129 prevented the disruption of a Caco-2 monolayer induced by pro-inflammatory cytokines. It increased transepithelial electrical resistance (TEER) and inhibited permeability induced by inflammation, along with an increased ZO-1 expression. Extracellular vesicles (EVs) from *P. freudenreichii* CIRM-BIA129, carrying the surface layer protein (SlpB), reproduced the protective effect of *P. freudenreichii* CIRM-BIA129. A mutant strain deleted for *slpB* (ΔslpB), or EVs from this mutant strain, had lost their protective effects, and worsened both DSS-induced colitis and inflammation *in vivo*.

These results shown that *P. freudenreichii* CIRM-BIA129 daily consumption has the potential to greatly alleviate colitis symptomss and, particularly, to counter intestinal epithelial permeability induced by inflammation by restoring ZO-1 expression through mechanisms involving S-layer protein B. They open new avenues for the use of probiotic dairy propionibacteria and/or postbiotic fractions thereof, in the context of gut permeability.

NEW :
1. *P.freudenreichii* reduces DSS-induced intestinal permeability *in vivo*
2. *P.freudenreichii* does not inhibit inflammation but damages linked to inflammation
3. *P.freudenreichii* inhibits intestinal epithelial breakdown through S-layer protein B

NOTEWORTHY :
1. The protective effects of *P.freudenreichii* depends on S-layer protein B
2. Extracellular vesicles from P. freudenreichii CB 129 mimic the protective effect of the probiotic

KEYWORDS
probiotic, inflammation, permeability, intestinal epithelium, zonula occludens-1

1. Introduction

Inflammatory bowel diseases (IBD) constitute a heterogeneous group of chronic inflammatory diseases including ulcerative colitis (UC) and Crohn's disease (CD), with a growing prevalence worldwide (Alatab et al. 2020). It involves immune response dysregulations, alterations of the enteric nervous system, gut microbiota dysbiosis, and intestinal epithelial barrier dysfunctions (Lê et al. 2022). Indeed, IBD patients exhibit aberrant immune responses such as infiltration of CD4+ T lymphocytes in the intestine, associated with a reduction in regulatory T (Treg) cells (Tindemans et al. 2020). The expression of enteric neuronal and glial markers is altered (Prigent et al. 2019; 2020; Le Berre et al. 2023) and glial cells have lost their functions in patients with CD (Pochard et al. 2016; Coquenlorge et al. 2016). In addition, a dysbiosis of the gut microbiota, characterized by a reduced bacterial diversity and alterations in the relative abundance of certain species were observed (Lê et al. 2022). At last, the intestinal epithelial barrier (IEB), serving as the first line of defense against the external environment, is failing. Indeed, there is increasing recognition of an association between disrupted IEB function and the development of inflammatory diseases. An increase in intestinal permeability occurs in IBD patients (Peeters et al. 1994; Pearson et al. 1982) and first-degree relatives of IBD patients (Munkholm et al. 1994). Increased permeability is often observed prior to relapse of CD (Wyatt et al. 1993). It is an aggravating factor in IBD, and the severity of symptoms is positively correlated with its extent (Chang et al. 2017). If increased permeability precedes inflammation (Arrieta et al. 2006), during inflammation, further barrier dysfunction can be induced by cytokines such as interferon-ɣ (IFN-ɣ) and tumor necrosis factor-α (TNF-α). This process is accompanied by changes in expression and/or redistribution of tight junction proteins such as the Zonula Occludens-1 (ZO-1), the occludin or the Claudin-2 (Turner et al. 2009). Interestingly, reducing barrier permeability prevents the development of inflammation in a genetic model of IBD (Arrieta et al. 2006). The strengthening or the re-establishment of IEB functions could therefore be interesting targets for approaches aiming at both prevention of relapses, and treatment of IEB-associated IBD dysfunctions.

Currently, the mainstays of IBD treatment are immunosuppressive and immune-modulating agents, and even protective functional foods are tested and developed for their anti-inflammatory properties (Lê et al. 2022). Beneficial bacteria, either ingested or members of the gut microbiota, may modulate gut inflammation through immunomodulation, engagement of an immune response and modulation of cytokines and of T-cells proliferation (Illikoud et al. 2022). Meta-analysis of clinical trials revealed the efficacy of selected probiotic strains, such as those constituting the VSL#3 product, in the context of IBD, while other strains failed to do so (Sniffen et al. 2018). In this context, promising immunomodulatory properties were reported for *Propionibacterium freudenreichii (P. freudenreichii),* an actinobacterium found in Swiss-type cheese, which holds a Generally Recognized as Safe (GRAS) status in the United States, as well as a Qualified Presumption of Safety (QPS) status in Europe. *P. freudenreichii* was shown to induce the modulatory cytokine IL-10 in human peripheral blood mononuclear cells, to mitigate the severity of TNBS-induced colitis and to counteract colonization of mice digestive tract by the rodent pathogen *Citrobacter rodentium* (Foligné et al. 2010). This property is highly *P. freudenreichii* strain-specific (Foligné et al. 2013), and depends on the presence of key surface layer proteins (Le Marechal et al. 2015), including SlpB, a main microbe-associated molecular patterns (MAMPs) involved in immunomodulation (Deutsch et al. 2017). In line with this, expression of *P. freudenreichii slpB* gene in *Lactococcus lactis* enhanced its ability

to mitigate DSS-induced colitis in mice, further indicating the key role of the SlpB protein (Belo et al. 2021). More recently, *P. freudenreichii* was shown to prevent the inflammatory damages caused by the cancer chemotherapy drug 5-fluorouracyl, while the *slpB* mutant failed to do so. In this mucositis model, the wild-type *P. freudenreichii* reduced the dramatic increase in gut permeability which was induced by 5-fluorouracyl (do Carmo et al. 2019). SlpB is also involved in *P. freudenreichii* adhesion to intestinal HT-29 epithelial cells (do Carmo et al. 2017) suggesting that *P. freudenreichii* could exert a protective effect towards the gut epithelial barrier.

We thus investigated whether *P. freudenreichii* could mitigate mice colitis and in particular protect the intestinal epithelial barrier from damages induced by inflammation. We paid special attention to its protective effect towards tight junctions, and have analysed the involvement of the *P. freudenreichii* surface layer protein SlpB.

2. Materials and methods

Growth of dairy propionibacteria

The strain *Propionibacterium freudenreichii* CIRM-BIA 129 (*P. freudenreichii* CIRM-BIA129), was initially isolated from a Swiss-type cheese. It was provided by CNIEL (Centre National Interprofessionel de l'Economie Laitière) and maintained by the CIRM-BIA microbiological ressource center (Centre International de Ressources Microbiennes, Bactéries d'Intérêt Alimentaire, Rennes, France). Starting from a frozen stock, precultures were grown in liquid Yeast Extract Lactate (YEL) medium containing 0.1 M sodium DL-lactate (Sigma Aldrich, Saint Louis, USA) and 10 g/L yeast extract as described (Malik et al. 1968). *P. freudenreichii* CIRM-BIA129 was then grown at 30°C for 60 hours in milk ultra-filtrate (MUF) supplemented with 5 g/L casein peptone (casein peptone plus, Organotechnie, La Courneuve, France), 0.1M sodium DL-lactate filter-sterilized using a 0.2 µm NalgeneTop filter (Sigma-Aldrich, St. Louis, MO, USA). Propionibacteria were grown in agar-solidified media in anaerobic jars containing ATCO Biocult anaerobiosis generators (Laboratoires Standa, Cean, France). They were grown in liquid media in microaerophilic conditions in glass tubes with screw cap (2 thirds of volume occupied by liquid medium, one third by headspace air), at 30°C, without agitation. Regarding the knock-out strain *P. freudenreichii* CIRM-BIA129Δ*slpB*, YEL and MUF culture media were supplemented with chloramphenicol (10 µg/mL) as previously detailed in (do Carmo et al. 2018). For Caco-2 cells stimulation (see below), propionibacteria were centrifuged (10,000 x *g*, 10 min, 20°C), and resuspended in DMEM medium prior to addition to cell cultures.

DSS-induced colitis, *in vivo* DAI and permeability assessment

Eight-week-old C57Bl/6NRj male mice from Janvier Labs (Le Genest St Isle, France) were housed in a ventilated cage system under a 12-hours light-dark cycle and ad libitum access to food (SAFE A04) and drinking water. The experiments were carried out in strict accordance with the European Communities Council Directives 2010/63/UE on the use of laboratory animal. Mice were randomly divided into 4 groups of 14 animals: MUF, 129, DSS and 129DSS. Mice were gavaged daily either with 200 µL of MUF (MUF and DSS groups) or 200 µL of MUF fermented with *P. freudenreichii* CIRM-BIA129 at 1.10^8 CFU (129 and 129DSS groups) for 11 days. The last 4 days, colitis was induced by 4% (w/v) of Dextran Sulfate Sodium (DSS, colitis grade 36,000-50,000, MP Biomedicals, Eschwege, Germany) in drinking water renewed every day for the groups DSS and 129DSS. Animals were weighted daily and at the end of the protocol, mice received (5 µL/g of mouse) a solution comprising 30 mg/ml carmine red (cochineal carmine, Prolabo #22259), 10 mg/mL fluorescein-5,6-sulfonic acid (FSA, fluorescein-5-(and-6)-sulfonic acid, trisodium, F1130, In vitrogen), 100 mg

Dextran TRITC (TRITC-dextran 4kDa, TdB Labs), and 10 mg/mL horseradish peroxidase (HRP; Peroxidase from horseradish, P8250, Sigma-Aldrich) resuspended in 0.5% carboxymethylcellulose in PBS (Sigma-Aldrich) *via* gavage, and then placed in individual cages. The Disease Activity Index (DAI) was determined as indicated in **Table 1**, according to the 3 main clinical symptoms of colitis: diarrhea, rectal bleeding, and weight loss, following a scoring previously described (Cooper et al. 1993). Four hours after gavage, blood was collected from the tail vein and permeability was evaluated in 5 µL of plasma. Paracellular permeabilities were evaluated *via* titration of FSA and TRITC-dextran fluorescence intensity measured at 487 nm and 520 nm, respectively, using an automatic microplate reader (BioTek Synergy H1, microplate reader). Transcellular permeability to HRP was measured using an enzymatic activity assay with 3,3′,5,5′-tetramethylbenzidine reagent (TMB Substrate Reagent Set, 555214, BD Biosciences). Mice were killed at the end of the protocol by cervical dislocation. Colonic tissues were collected and snap frozen for further quantification of gene transcripts and of proteins, or were also fixed for 24 hours in 4% paraformaldehyde for histopathological analysis. This procedure was repeated 3 times independently.

Histopathological score

After fixations, distal colons were dehydrated and embedded in paraffin. Sections of 5 µm were stained with haematoxylin–phloxine–saffron (HPS) or Alcian Blue (MicroPICell platform, Nantes, France) for histopathological analysis. Images were taken using a slide scanner (Nanozoomer; Hamamatsu). As previously described, distal colonic tissue damage was evaluated by two investigators in a blinded manner through the calculation of a micro disease activity index (mDAI) which reflects the destruction of mucosal architecture, the cellular infiltration, muscle thickening and goblet cells depletion (Pochard et al. 2021). The scoring for the destruction of mucosal architecture was as follows: 0-3 (0: none, 1: 1/3 basal, 2: 2/3 basal, and 3: loss of crypt and epithelium). The extent of cellular infiltration was rated on a scale of 0-3 (0: none, 1: infiltrate around crypt basis, 2: extensive infiltration reaching the muscularis mucosae, and 3: infiltration of the submucosa). The degree of muscle thickening was also ranging from 0 to 3, when the thickening was none, mild, moderate, or extensive thickening, respectively. The loss of goblet cell depletion was scored as 0 (normal presence) or 1 (massive depletion). A multiplication factor of 1–4 was applied for each measured criteria, depending on the extent of affected area (25, 50, 75, or 100%) of the considered sample. Crypt length was considered by measuring the length of 50 opened crypts/animal.

Lipocalin-2 enzyme-linked immunosorbent assay faecal quantification

The feces of each mouse were resuspended in a solution of PBS-Tween 20 0.1% protease inhibitor cocktail (1/2 tablet for 25 mL solution, cOmplete; Roche, France) to reach 100 mg feces/mL. Lcn-2 in the faecal solution was measured using an enzyme-linked immunosorbent assay (ELISA) kit (Mouse Lcn-2/NGAL DuoSet ELISA; Bio-Techne), according to the manufacturer's protocol.

Caco-2 culture

The human IEC line Caco-2 was obtained from American Type Culture Collection (Manassas, VA) and cultured in Dulbecco modified Eagle medium containing 4.5 g/L glucose (Gibco, Life Technologies, Carlsbad, CA) supplemented with 10% heat-inactivated fetal calf serum, 2 mmol/L glutamine, 100 IU/mL penicillin, and 100 µg/mL streptomycin. For treatments, transepithelial electrical resistance (TEER) and permeability experiments, 116.071 cells/cm^2 were seeded onto Transwell Permeable Supports (Costar, REF 3460) and grown for 21 days.

Guanidine extraction and purification of surface layer proteins

Propionibacteria were cultivated in MUF as described above and harvested in late stationary phase, after 72 hours of culture. They were then harvested by centrifugation (10,000 x *g*, 10 min, 20°C), washed in PBS and resuspended in 5 M guanidine hydrochloride (20% of the initial culture volume). The bacterial suspension was incubated 15 min at 50°C prior to centrifugation (20,000 x *g*, 20 min, 20°C). The supernatant was then extensively dialyzed against distilled water (20 L) and then against PBS (5 L) using a Slide-A-Lyzer Dialysis Cassette (Thermo Scientific) with a 10 kDa Cut-Off.

Purification of EVs and Nanoparticle Tracking Analysis for EV size and concentration determination.

To extract and purify extracellular vesicles derived from *P. freudenreichii* CIRM-BIA129 and from its Δ*slpB* isogenic mutant (*P. freudenreichii* CIRM-BIA129 Δ*slpB*), the bacteria were pelleted by centrifugation (6,000 x *g*, 20 min, room temperature) of a 1 L culture and the supernatant fraction was filtered using a Nalgene 0.22 µm top filter (Thermo Scientific) to remove bacteria. Then, the supernatant was concentrated 1,000 times using Amicon ultrafiltration units with 100 kDa cut-off point through successive centrifugations at 2,500 g x *g*. The concentrated suspension of EVs was recovered in 500 µL of TBS buffer (Tris-Buffered Saline, 150 mM NaCl; 50 mM Tris-HCl, pH 7.5) prior to purification by size exclusion chromatography. Qevoriginal columns (qEV original 70 nm; iZON) were equilibrated with TBS and used according to the manufacturer's recommendations (Böing et al., 2014). The concentrated EV suspension (500 µL) was applied to the top of the chromatographic column and allowed to run into the column. 10 mL of TBS were then added on top of the column, prior to elution. Then, fractions of 500 µL were recovered in separate tubes. This chromatography step was conducted as previously described (Rodovalho et al. 2020) and EVs were reproducibly detected by NTA (see below) and by protein quantification in fractions 7 to 9. Finally, EVs-containing fractions (fractions 7-9) were pooled together, and the remaining fractions were discarded due to protein contamination or low EV content. To measure the size and concentration of EVs, nanoparticle tracking analysis (NTA) was performed at 25.0°C using a NanoSight NS300 instrument (Malvern Panalytical) with a CMOS camera and a Blue488 laser (Mehdiani et al., 2015). Samples were diluted to reach a concentration in the range 10^7 to 10^8 particles/mL, giving rise to 20 to 110 particles per frame. Samples were applied at 25°C in constant flux with a syringe pump speed of 50 µL/s. For each measurement, 5 x 60-s videos were recorded with camera level 15. Other parameters were adjusted accordingly to achieve image optimization.

Caco-2 treatments, TEER, and Permeability Measurement *In Vitro*

To determine the effect of propionibacteria, sodium-pyruvate (#11360070 ThermoFisherScientific), propionibacteria'supernatant, Slp, (enriched extracts of S-layer proteins), EVs or inflammation on intestinal epithelium, the TEER was measured before and after treatments with an epithelial voltohmmeter (EVOM; World Precision Instruments, Inc, Sarasota, FL). Caco-2 cells were stimulated for 24 hours with either *P. freudenreichii* CIRM-BIA129 or *P. freudenreichii* CIRM-BIA129Δ*slpB* (MOI 1:100), or S-layer protein enriched extracts (10-200 µg/mL), and EVs from *P. freudenreichii* CIRM-BIA129 or *P. freudenreichii* CIRM-BIA129Δ*slpB* at a concentration of 10^7 particles/mL in DMEM medium (0% FBS, 1% P/S) in the apical compartment or sodium-pyruvate (0.1-10 mM) in DMEM medium (10%FBS, 1% P/S) in the basolateral compartment. After 24 hours, an inflammatory stimulation was induced with a cytomix containing 50 ng/mL of TNF-α (human TNF-α, 50 µg, 130-094-017, Milteny Biotec) and 500 ng/mL of IFN-γ (human IFN-g1b, 1,000 µg, 130-

096-486, Milteny Biotec) in 0% FBS in the apical compartment as well as in 10% FBS in the basolateral compartment, for 6 days with a renewal on day 3. To determine the effect of these treatment on permeability, 50 µL of the apical medium was replaced by 50 µL of 1 mg/mL of sulfonic acid FITC, 6 mg/mL of dextran 4 kDa TRITC and 3 mg/mL of HRP. The fluorescence level of basolateral aliquots (150 µL) was measured every 30 min for a period of 180 min using a fluorimeter (BioTek Synergy H1, microplate reader). Paracellular permeability was determined by averaging the slope change in fluorescence intensity over time by linear regression fit model. To assess transcellular permeability to HRP (Peroxidase from horseradish, P8250, Sigma-Aldrich), an enzymatic activity assay with TMB (TMB Substrate Reagent Set, 555214, BD Biosciences, France) was performed.

mRNA and protein extractions

Proximal colons from mice were lysed in RA1 buffer (Macherey-Nagel) with the Precellys 24 tissue homogenizer (Bertin Technologies, Montigny-le-Bretonneux, France), and total RNA and protein extraction was performed with a Nucleospin RNAII kit according to the manufacturer's recommendations. For Caco-2 filters, cells were lysed in ice-cold RIPA Lysis buffer (20-188, Merk) complete with protease inhibitor (66373700, Merk), a phosphatase inhibitor cocktail (P0044, Sigma) and sodium orthovanadate (S6508, Sigma).

Quantitative real-time PCR analysis

One microgram of purified mRNA was denaturated and processed for reverse transcription using Superscript III reverse transcriptase (Life Technologies). qPCR amplifications were performed using FastSYBR Green Master Mix kit (Applied Biosystems, Foster City, CA, USA) and run on a StepOnePlus system (Life Technologies). The primers used are listed in **TABLE S2** (DOI 10.6084/m9.figshare.24542629). Ribosomal protein S6 (RPS6) transcript was used as a reference gene. The relative transcript level of the gene of interest was measured by the $2^{-\Delta\Delta Ct}$ method.

Western Blot

For proximal colon, proteins were resuspended in 1:1 protein solving buffer and tris(2-carboxyethyl) phosphine-reducing agent (PSB-TCEP, Macherey-Nagel), sonicated and denatured for 5 min at 95°C. For Caco-2 filters, cells were washed with ice-cold PBS and lysed in ice-cold 1X RIPA buffer complete with protease inhibitor (Roche, France) and serine-threonine phosphatase inhibitor (Sigma-Aldrich) cocktails and completed with NuPAGE™ LDS Sample Buffer 4X (NP0008, Invitrogen) and NuPAGE™ Sample reducing agent 10X (NP0009, Invitrogen), sonicated and denatured for 10 min at 70°C. Fifteen micrograms of proteins were separated using NuPAGE™ 4-12% Bis-Tris or NuPAGE™ 3-8% Tris-Acetate gels (Life Technologies, Villebon sur Yvette, France) and transferred to nitrocellulose membranes (Life Technologies, Villebon sur Yvette, France). After blocking with Tris-buffered saline/0.1% Tween-20/5% nonfat dry milk for 30 min, blots were incubated overnight at 4°C with the primary antibodies (**Table S1**, DOI 10.6084/m9.figshare.24542629) diluted in Tris-buffered saline/5% nonfat dry milk.

Immunoblots were probed with HRP-conjugated anti-rabbit (Life technologies, 1:5,000) or anti-mouse secondary antibodies (Sigma, 1:5,000) and visualized by chemiluminescence (Clarity Western ECL Substrate, 170-5061, BioRad or Femto Maximum Sensitivity Substrate, 34095, Thermofisher) using a ChemiDoc MP Imaging System (Bio-Rad). Western Blot data are expressed as relative values to ß-actine and normalized to the control mean.

Organic acid quantification

To identify whether soluble mediators are responsible for the *P. freudenreichii* CIRM-BIA129 effects dependent on the SlpB protein on the Caco-2 barrier, organic acids present in the apical and basolateral culture media at the end of the IEB-disruption protocol were analysed by High Performance Liquid Chromatography UltiMate 3000 (HPLC, Thermofisher, Les Ulis, France). Culture media were diluted 2-fold in 0.005 M H_2SO_4, prior to centrifugation (7500 × *g* for 15 min at 4 °C), and filtration (chromafil Xtra PVDF 45/13, Macherey Nagel, Düren, Germany). HPLC analysis was then conducted using a Rezek ROA organic acid H + column (300*7.8 mm, Phenomenex, California), with 0.005 M NH_2SO_4 as mobile phase, and a flow rate of 0.4 mL/min at 60°C. A UV detector (DIONEX-UVD 170U, Sunnyvale, California) operating at 210 nm, as well as a refractometer (RI 2103 Plus Jasco, Tokyo, Japan) were used. External calibration was used for quantification. Standards of lactic, citric, propionic, butyric, succinic, and pyruvic acids were purchased from Merck (St. Quentin Fallavier, France, and acetic acid from PanReac, Lyon, France).

Statistical analysis

Results were expressed as mean +/- SEM. Outliers were excluded using Grubbs' tests. Statistical significance was analyzed by an ordinary two-way ANOVA, followed by a Tukey's multiple comparisons test, with a single pooled variance or a Kruskal-Wallis test, followed by a Dunn's multiple comparisons test (GraphPad Prism 9). Differences between experimental groups were considered significant at *p<=0.05, ** p<=0.01, *** p<=0.001 or p<=0.0001.

3. Results

***P. freudenreichii* CIRM-BIA129 reduces DSS-induced colitis severity and intestinal permeability *in vivo*.**

For *in vivo* assessment of *P. freudenreichii* CIRM-BIA129 ability to prevent colitis, acute colitis was induced by the addition of 4% DSS for 4 days to the drinking water of 8–10-weeks-old male supplemented, or not, with the *P. freudenreichii* CIRM-BIA129 for 11 days (Figure 1A). The colitis was characterized by an increased disease activity index (DAI) in the DSS as well as in the 129DSS groups compared to the MUF group (Figure 1B), but *P. freudenreichii* CIRM-BIA129 supplementation (129DSS group) significantly reduced the DAI score by about 50% compared to the DSS group (Figure 1B). The DAI was composed of three parameters: the bleeding and the stool consistency scores, and the weight change. *P. freudenreichii* CIRM-BIA129 supplementation inhibited DSS-induced increase in bleeding and stool consistency scores, but did not change the weight loss (Suppl Fig 1 ; DOI 10.6084/m9.figshare.24542629). The paracellular permeability measured *in vivo* by sulfonic acid (0.4 kDa) passage in mice plasma was also increased in the DSS and in the 129DSS groups compared to the MUF group, but again significantly less in the 129DSS group than in the DSS group (Figure 1C). The transcellular permeabilities measured *in vivo* by HRP (44 kDa) in mice plasma tended to be increased in the DSS group (p-value=0.0653) and was significantly lower in the 129DSS compared to the DSS group (Figure 1D). The histopathological score, reflecting the remodeling of the distal colon (cellular infiltration, muscle thickening, epithelial destruction), was significantly increased in the DSS as well as in the 129DSS groups compared to the MUF group (Figures 1E and F). The crypt length was reduced in the DSS group but not when mice were supplemented with the *P. freudenreichii* CIRM-BIA129 (Figure 1G). Under basal conditions, *P. freudenreichii* CIRM-BIA129 supplementation has had no impact on the measured parameters (Figures 1B-G). Altogether, these results show that *P. freudenreichii* CIRM-BIA129 is safe and has the potential to alleviate the severity of colitis and to maintain intestinal barrier function such as permeability.

348

349 ***P. freudenreichii* CIRM-BIA 129 promotes ZO-1 protein remodeling without reducing**
350 **inflammation.**

351 To investigate in more details whether *P. freudenreichii* CIRM-BIA129 supplementation
352 impacted the intestinal epithelium and/or inflammatory processes, the amount of tight
353 junctions (TJ) proteins, as well as of inflammatory cytokines, were evaluated in the mice
354 proximal colons and the release of a marker of intestinal injury (fecal concentration of Lcn-2
355 for neutrophil gelatinase-associated Lcn) was measured in stools. Western-blot analyses have
356 shown that *P. freudenreichii* CIRM-BIA129 supplementation significantly increased the
357 expression of the Zonula Occludens-1 (ZO-1) in the absence of colitis and through a tendency
358 under DSS-induced colitis conditions with a noticeable variability within the samples (Figure
359 2A, 2B). Neither DSS nor 129 has modified the expression of occludin, another TJ protein
360 (Figure 2A, 2C). Regarding the expressions of genes encoding pro- and anti-inflammatory
361 cytokines, DSS treatment significantly up-regulated the level of *il-1ß* transcripts and tended to
362 decrease *il-10* ones (Figure 2D, 2F), but had no impact on *tnf-α* transcripts (Figure 2E). Fecal
363 Lcn-2 concentration was increased in the DSS and 129DSS groups compared to the MUF
364 group (Figure 2G). *P. freudenreichii* CIRM-BIA129 supplementation did not modify these
365 markers, neither in control, nor in DSS condition (Figures 2D, 2E, 2F, 2G). Overall, these
366 findings support the hypothesis that *P. freudenreichii* CIRM-BIA129 mitigates the severity of
367 DSS-induced colitis through its action on IEB, and in particular ZO-1 expression, rather than
368 on inflammation.

369

370 ***P. freudenreichii* CIRM-BIA 129 inhibits inflammation-induced IEB breakdown**
371 **through S-layer protein B induction of ZO-1 expression.**

372 To analyse more specifically the regulation of intestinal epithelium permeability by the
373 propionibacteria, an *in vitro* IEB model was challenged with inflammation with or without
374 pre-treatment with the *P. freudenreichii* CIRM-BIA129 (Figure 3A). As *P. freudenreichii*
375 CIRM-BIA129 anti-inflammatory effects (do Carmo et al. 2019) and it's adhesion to HT29
376 colonic cells (do Carmo et al. 2017) involved the S-layer protein B (SlpB), an isogenic mutant
377 deleted for the *slpB* gene (*P. freudenreichii* CIRM-BIA129Δ*slpB*) was also tested in this
378 protocol. After 24 hours of incubation with the bacteria and a full culture medium
379 replacement, *P. freudenreichii* CIRM-BIA129 adhesion to Caco-2 monolayer was observed
380 using Gram staining (Figure 3B). This adhesion was greatly reduced when using the *P.*
381 *freudenreichii* CIRM-BIA129 Δ*slpB* (Figure 3B). No living bacteria have been observed at
382 the end of the protocol (data not shown). Without inflammation, *P. freudenreichii* CIRM-
383 BIA129 significantly lowered TEER compared to untreated cells, but has no impact on
384 permeabilities (Figures 3C, 3D, 3E). After 6 days, inflammation significantly reduced the
385 TEER (Figure 3C), increased the paracellular permeability to sulfonic acid-FITC (Figure 3D)
386 and increased the transcellular permeability to HRP (Figure 3E). Pre-incubation with the *P.*
387 *freudenreichii* CIRM-BIA129 prevented these three changes (Figures 3C, 3D, 3E). In
388 contrast, *P. freudenreichii* CIRM-BIA129 Δ*slpB* failed to inhibit these inflammation-induced
389 IEB failures (Figures 3C, 3D, 3E), and even increased the permeabilities induced by
390 inflammation (Figures 3D, 3E). To investigate the molecular mechanisms sustaining these
391 effects, the expressions of TJ proteins such as ZO-1 and occludin were analysed by western-
392 blot. Inflammation significantly reduced both ZO-1 and occludin protein expression, while *P.*
393 *freudenreichii* CIRM-BIA129 prevented the decrease of ZO-1 expression induced by
394 inflammation but had no effect on occludin expression (Figures 3F, 3G, 3H). Conversely, *P.*
395 *freudenreichii* CIRM-BIA129 Δ*slpB* was unsuccessful in restoring ZO-1 expression (Figures
396 3F, 3G). Taken together, these data provide evidence that *P. freudenreichii* CIRM-BIA129

inhibits IEB breakdown induced by inflammation by maintaining ZO-1 expression in a SlpB dependent manner.

Organic acid productions do not explain the *P. freudenreichii* protective effect on inflammation-induced IEB breakdown.

To assess whether soluble factors such as short chain fatty acids could be involved in SlpB-dependent effect of *P. freudenreichii* CIRM-BIA129 upon intestinal epithelium, organic acid concentrations were measured in the apical (Figure 4A) and basolateral (Figure 4B) compartments of our *in vitro* model of inflammation-induced IEB disruption. Acetate and propionate concentrations are increased by *P. freudenreichii* CIRM-BIA129 Δ*slpB* but not *P. freudenreichii* CIRM-BIA129 in apical and basolateral compartments without impact of inflammation (Figures 4A and 4B). Glucose concentrations were decreased by *P. freudenreichii* CIRM-BIA129, *P. freudenreichii* CIRM-BIA129 Δ*slpB* or inflammation in apical and basolateral compartments (Figure 4A and 4B). Inflammation-induced lactate concentrations are inhibited by *P. freudenreichii* CIRM-BIA129 Δ*slpB* in apical and basolateral compartments (Figures 4A and 4B). Inflammation-induced decreased 2-pyrrolidone-5-carboxylic acid concentration is decreased by *P. freudenreichii* CIRM-BIA129 or *P. freudenreichii* CIRM-BIA129 Δ*slpB* in apical compartment and increased by *P. freudenreichii* CIRM-BIA129 Δ*slpB* in the basolateral compartments (Figures 4A and 4B). Pyruvate concentration in the apical compartment was increased by *P. freudenreichii* CIRM-BIA129 or *P. freudenreichii* CIRM-BIA129 Δ*slpB* and only by *P. freudenreichii* CIRM-BIA129 in the basolateral compartment (Figures 4A and 4B). None of the concentrations were correlated with the changes of permeability observed, but as pyruvate concentrations were increased in basolateral compartment by *P. freudenreichii* CIRM-BIA129 but not *P. freudenreichii* CIRM-BIA129 Δ*slpB*, we have tested if it could contribute to *P. freudenreichii* CIRM-BIA129 inhibition of inflammation-induced permeability. None of the tested concentrations were efficient in modulating Caco-2 permeability (Figure 4C). Beyond SCFAs, *P. freudenreichii* CIRM-BIA129 has the ability to generate other soluble mediators. To investigate the potential involvement of the bacterial-released soluble mediators, we evaluated *P. freudenreichii* CIRM-BIA129 supernatant in our *in vitro* model. The supernatant did not exhibit any protective effect against the inflammation-induced increase in permeability (Figure 4D). These data suggest that SlpB-dependent effect of *P. freudenreichii* CIRM-BIA129 upon epithelial permeability does not involve soluble mediators released by the bacteria.

Extracellular vesicles from *P. freudenreichii* CIRM-BIA 129 containing the SlpB protein are efficient to inhibit inflammation-induced IEB breakdown

To further explore the direct contribution of SlpB in reinforcing the IEB, enriched extracts of S-layer proteins (Slp) were tested in our *in vitro* model of inflammation-induced IEB disruption. Various concentrations of Slp, ranging from 10 µg/mL to 200 µg/mL, failed to inhibit the increase in paracellular permeability induced by inflammation, that remained significantly increased except for high concentration (Figure 5A). Nevertheless, this method is insufficient to conclude about the inability of isolated SlpB to modulate the permeability, as (i) guanidine chloride extraction samples also contain other proteins, and (ii) Slps are poorly soluble, forming aggregates in aqueous environments (do Carmo et al. 2018). Therefore we produced and tested extracellular vesicles (EVs) from *P. freudenreichii* CIRM-BIA129 that are known to contain the well-conformed SlpB protein (Rodovalho et al. 2020), and compared their effects to that of EVs produced from strain *P. freudenreichii* CIRM-BIA129 Δ*slpB*. The productions of EVs were verified by nanoparticle tracking analysis (NTA) to control the similar size profile and adjust the concentrations before treating Caco-2 cells (Figures 5B and

5C). EVs derived from *P. freudenreichii* CIRM-BIA129, but not from *P. freudenreichii* CIRM-BIA129 Δ*slpB*, successfully inhibited the increase in paracellular permeability to sulfonic acid-FITC caused by inflammation (Figure 5D). These findings highlight the essential role of SlpB in barrier protection by *P. freudenreichii* CIRM-BIA129.

Deletion of SlpB surface protein exacerbates colitis.

To confirmed the necessity of SlpB in *P. freudenreichii* CIRM-BIA129 protective effect *in vivo*, induction of colitis was induced by DSS in mice supplemented with *P. freudenreichii* CIRM-BIA129 Δ*slpB*. The mutant strain had no effect on DAI score increased by DSS (Figure 6A). It exhibited a tendency to raise paracellular permeability to sulfonic acid-FITC compared to DSS condition (Figure 6B) and significantly elevated the transcellular permeability to HRP compared to the DSS condition (Figure 6C). Moreover, *P. freudenreichii* CIRM-BIA129 Δ*slpB* did not changed the level of *il-1ß* transcripts and exacerbated the increase in transcript levels of *tnf-α* mRNA induced by DSS (Figures 6D and 6E). Surprisingly, *il-10* transcripts were increased in the presence of *P. freudenreichii* CIRM-BIA 129Δ*slpB* compared to the DSS condition (Figure 6F). These data show *slpB* deletion not only abrogated *P. freudenreichii* CIRM-BIA129 protection but also exacerbated colitis through an increased inflammation and permeability.

4. Discussion and conclusion

Disruption of intestinal epithelial barrier (IEB) plays a central role in the pathogenesis of IBD and stands as a pivotal target for effective IBD therapies (Chang et al. 2017). This study demonstrated that the anti-inflammatory dairy bacterium *P. freudenreichii* CIRM-BIA129 strain can counter inflammation-induced barrier disruption *in vitro* and *in vivo*. It revealed that through the expression of the surface protein SlpB, the *P. freudenreichii* CIRM-BIA129 maintains the expression of the tight junction protein ZO-1, thereby strengthening the IEB *in vitro* and *in vivo*.

P. freudenreichii is widely recognized for its anti-inflammatory properties (do Carmo et al. 2019; Ma et al. 2020), both *in vitro* and *in vivo*, through the regulation of immune cells but also epithelial cells. Indeed, probiotic bacteria can interact with dendritic cells and with intestinal epithelial cells, leading to anti-inflammatory effects of specific strains (Sniffen et al. 2018). *P. freudenreichii* enhances the production of IL-10 by human peripheral blood mononuclear cells and reduces the levels of TNF-α and IL-8 induced by lipopolysaccharide stimulation of epithelial HT-29 cells (do Carmo et al. 2019; Foligné et al. 2010). In the present study, *P. freudenreichii* CIRM-BIA129 exerted no significant effect on inflammation *in vivo* in a mice model of acute colitis, but had a major impact upon the gut barrier function. *P. freudenreichii* CIRM-BIA129 was shown to specifically target the intestinal epithelium to enhance one of its major function, the control of permeability. This complements previous studies showing the adhesion of *P. freudenreichii* CIRM-BIA129 to HT-29 cells and describing its capacity to protect the IEB in a mucositis model (do Carmo et al. 2019). Other probiotic such as *Lactiplantibacillus plantarum* (formely *Lactobacillus plantarum*) may also protect the intestinal epithelial barrier through the regulation of the expression of key tight junction proteins such as claudin-1, occludin, and ZO-1 (Wang et al. 2018). *P. freudenreichii* CIRM-BIA *129* can also enhance the mRNA expression of ZO-1 (Deutsch et al. 2017; Le Maréchal et al. 2015; Rabah et al. 2018; do Carmo et al. 2017) and we have further demonstrated here that *P. freudenreichii* CIRM-BIA129 also induces ZO-1 protein expression.

The IEB cytoskeletal integrity, survival and apoptosis are regulated by probiotics through key bacterial surface components named microbe-associated molecular patterns

(MAMPs), which are recognized by corresponding host pattern recognition receptors (PRR) (Lebeer et al. 2010) as well as soluble factors (Capurso et al. 2019; Yan et al. 2012). The mechanism by which *P. freudenreichii* strengthens IEB seems to exclude soluble factors, as bacterial supernatants did not reproduce the bacterial effect, and none of the organic acid present in apical or basolateral epithelial sides were correlated with the permeability observed. Surprisingly, the supernatant contains EVs, although in all likelihood, their quantity is insufficient to mediate the protective effects of *P. freudenreichii.* However, we have demonstrated that *P. freudenreichii* CIRM-BIA129 adheres to Caco-2 cells, and induces ZO-1 protein expression in a SlpB-dependent manner. It should be noted that this *in vitro* effect relies on propionibacteria and on their surface components, yet not on an active metabolism, which is not possible in the conditions of these *in vitro* co-incubations. Other bacterial probiotic species, including lactobacilli, were already shown to possess surface layer proteins involved in probiotic/host interactions. As an example, *Lactobacillus acidophilus* binds to dendritic cells C-type lectin SIGNR3 and, regulates immature dendritic cells and T cells functions, mitigating gut inflammation as well as mucosal barrier function in mice, thanks to a specific surface layer protein (Konstantinov et al. 2008; Lightfoot et al. 2015). We previously showed that SlpB was involved in and necessary to the *P. freudenreichii* probiotic effect (Deutsch et al. 2017; Le Maréchal et al. 2015; Rabah et al. 2018; do Carmo et al. 2017). Herein, we focused our study on IEB and showed that SlpB reinforces the barrier, as strain lacking *slpB* gene have lost their protective effect upon inflammation-induced IEB disruption. However, it is important to acknowledge that the mutant strain exhibits pleiotropic effects on the bacteria itself (do Carmo et al. 2018). In the present study, in addition to the loss of SlpB, we evidenced the remodeling induced by SlpB deletion through the major change induced in organic acid productions. The increased production of acetate and propionate by the *P. freudenreichii* CIRM-BIA129 Δ*slpB* in comparison to the wild type strain *P. freudenreichii* CIRM-BIA129 could explain the aggravating effect of the bacteria upon permeability and inflammation. But to focus and identify whether isolated SlpB could be responsible of the probiotic effect of *P. freudenreichii* CIRM-BIA129, we have treated epithelial monolayer with a guanidine extract enriched in *P. freudenreichii* surface layer proteins, but it had no effect. This observation does not imperatively mean that isolated SlpB are not enough to induce the probiotic effect, but rather than SlpB, although it is not a transmembrane protein, must interact with a lipid bilayer to be well conformed and operational. Slps are known for their capacity to aggregate, after extraction, forming paracrystalline structures different in the guanidine extract than on the surface of propionibacteria envelope (do Carmo et al. 2018). In a consistent manner, the heterologous expression of *slpB* in *Lactococcus lactis* NCDO 2118 that confers probiotic potential to the strain to alleviate DSS-induced colitis in mice (Belo et al. 2021).

Our work mainly observed the regulation of the IEB by *P. freudenreichii*, shedding light on the significant role of epithelium dysfunction into colitis development. However, it is equally surprising to note the absence of any discernible anti-inflammatory effects, emphasizing the crucial role of the matrix. Indeed, we have already demonstrated the role of the dairy matrix in the modulation of *P. freudenreichii* probiotic activity. The cheese matrix was shown to protect the immunomodulatory SlpB protein from digestive proteolysis (Rabah et al. 2018), and the presence of dairy fat in the fermented product potentiates the anti-colitis effects of the probiotic strain (Mantel et al. 2023). In the present work we gave *P. freudenreichii* in milk ultra-filtrate supplemented with casein peptone and sodium DL-lactate, that seems unsuitable to support anti-inflammatory effect. Further studies are necessary to determine to which extend the matrix composition is crucial for the bacterial strain, or for the host, to obtain optimal effects. Another strategy could be to deliver and to trigger of the probiotic effects in a matrix-independent-way. Our study also shows that EVs

are efficient vehicles to mimic the protective effect of *P. freudenreichii* upon inflammation-induced IEB disruption. They have previously been shown to reduce inflammation in cultured human intestinal cells by modulating the NF-κB pathway (Rodovalho et al. 2020), and could be efficient to protect the IEB as well as to damper inflammation. It opens new avenues for the definition of preventive strategies against chronic diseases involving intestinal barrier hyperpermeability and inflammation, avoiding the drawbacks associated with the use of live bacteria.

Finally, the research work presented here was performed on model systems which are still distant from clinical situations. The Caco-2 cell line is a cancer cell line different from healthy human colon epithelial cells and DSS-colitis in mice only mimics inflammatory conditions. However, this work, in addition to previous data using human PBMCs, HT-29 cells, Caco-2 cells, TNBS-colitis, DSS- colitis and 5-FU mucositis constitute a body of converging indications pointing at the anti-inflammatory potential of selected strains of *P. freudenreichii*. Pilot clinical studies further suggest the interest of this probiotic bacterium in the context of inflammatory conditions (Suzuki et al. 2006). However, further clinical investigations are needed to precise the future use of propionibacteria in live biotherapeutic applications.

ACKNOWLEDGMENTS

This work was supported by the « Institut national de la santé et de la recherche médicale » (Inserm), the Nantes Université and the cluster IBD NExt from Nantes Excellence Trajectory (NExT Health & Engineering) and the "Institut national de recherche pour l'agriculture, l'alimentation et l'environnment" (INRAE). MM benefits a doctoral fellowship managed by Bba Milk Valley, dairy industrial association. We are grateful to Regional Councils of Bretagne (grant no. 19008213) and Pays de la Loire (grant no. 2019-013227) for their financial support through the interregional project PROLIFIC. MRD is supported by the Centre National pour la Recherche Scientifique (CNRS). Figures were created with BioRender.com. Authors thank Nicodème Hent'al for usefull advices.

LEGENDS TO THE FIGURES

Figure 1. *P. freudenreichii* CIRM-BIA129 mitigates DSS-induced colitis severity and reduces intestinal permeability *in vivo*. (A) Eight-week-old C57BL6 mice were gavaged during 11 days with milk ultra-filtrate (MUF) or MUF fermented by *P. freudenreichii* CIRM-BIA129(129) containing 1.10^8 CFU. At day 7, 4% DSS was added to drinking water or not. On day 11, permeabilities were measured, mice sacrificed, and the tissues collected. (B) Disease activity index (DAI) of the 4 groups: control (MUF) or *P. freudenreichii* CIRM-BIA129 (129) in control conditions (grey) or with DSS (DSS and 129DSS in orange) at day 11. (C) Paracellular and (D) transcellular permeabilities evaluated by measurement of sulfonic acid and HRP in animal plasma 4 hours after mice gavage, respectively. (E) Representative images of Alcyan Blue staining of the distal colon. (F) Histological scores (mDAI) quantifying the destruction of mucosal architecture, cellular infiltration, muscle thickening and loss of goblet cells. (G) Crypts length measured for 50 opened crypts per animal. Data represent mean +/- SEM of 14 mice per group.

Figure 2. *P. freudenreichii* CIRM-BIA 129 promotes tight junction protein remodeling without reducing inflammation. (A) Representative Western blot analysis of ZO-1, occludin (OCLN) and ß-actin. (B) Quantification of ZO-1, and (C) occludin expression normalized to β-actin and relative to control mean. Quantification of transcript levels of (D) *il-1ß*, (E) *tnf-α,* and (F) *il-10* measured at day 11 in the proximal colon of the four groups. Relative expression

was determined using *Rps6* as reference gene. Both protein and transcript levels were normalized to control mean. (G) Fecal lipocalin contents were measured at day 11.

Figure 3. *P. freudenreichii* CIRM-BIA129 inhibits inflammation-induced IEB breakdown through S-layer protein B induction of ZO-1 expression. (A) Caco-2 cells grown on transwell for 21days were left untreated or pre-treated with *P. freudenreichii* CIRM-BIA129 or *P. freudenreichii* CIRM-BIA129 Δ*slpB* (MOI 100:1) for 24 hours before removal and treatment with an inflammatory cytomix containing TNF-α and IFN-ɣ was added for 6 days, with a renewal at day 3. (B) Gram staining of *P. freudenreichii* CIRM-BIA129 culture. The top-left image showed the bacteria in its fresh state; top right showed Caco-2 cells without any bacteria were the pore filter are visible; down-left, Caco-2 cells after 24hours with *P. freudenreichii* CIRM-BIA129; down-right, Caco-2 cells after 24hours with *P. freudenreichii* CIRM-BIA129 Δ*slpB*. (C) Trans-epithelial electrical resistances (TEER), (D) Sulfonic acid-FITC diffusion (E) HRP diffusion were measured at the end of the experiment. (F) Representative western blot analysis of ZO-1, occludin (OCLN) and ß-actin amounts. (G) Quantification of ZO-1 and (H) OCLN expressions normalized to β-actin and relative to control mean (Ct grey). Values are expressed as means +/- SEM.

Figure 4. Organic acid productions do not explain the *P. freudenreichii* CIRM-BIA129 protective effect on inflammation-induced IEB breakdown. Caco-2 cells grown on transwell for 21 days were left untreated or pre-treated with *P. freudenreichii* CIRM-BIA129 or *P. freudenreichii* CIRM-BIA129 Δ*slpB* for 24 hours before removal and treatment with an inflammatory cytomix containing TNF-α and IFN-ɣ was added for 6 days, with a renewal at day 3. Impact of *P. freudenreichii* CIRM-BIA129 or *P. freudenreichii* CIRM-BIA129 Δ*slpB* on the concentrations of different SCFAs was measured (A) at the apical and (B) basolateral compartments at the end of the experiment. Caco-2 cells grown on transwell for 21days were left untreated or pre-treated with the indicated concentrations of sodium-pyruvate at the basolateral side for 24 before removal and treatment with an inflammatory cytomix described above was added for 6 days, with a renewal at day 3. (C) Sulfonic acid-FITC diffusion was measured at the end of the experiment. Caco-2 cells were left untreated or pre-treated with the *P. freudenreichii* CIRM-BIA129's supernatant for 24 h before removal, and treatment with an inflammatory cytomix described above was added for 6 days, with a renewal at day 3. (D) Sulfonic acid-FITC diffusion was measured at the end of the experiment. Data are expressed as means +/- SEM.

Figure 5. Extracellular vesicles from *P. freudenreichii* CIRM-BIA 129 containing the SlpB protein are efficient to inhibit inflammation-induced IEB breakdown. Caco-2 cells grown on transwell for 21days were left untreated or pre-treated with the indicated concentrations of S-layer protein extracts from *P. freudenreichii* CIRM-BIA129 for 24h before removal and treatment with an inflammatory cytomix containing TNF-α and IFN-ɣ was added for 6 days, with a renewal at day 3. (A) Sulfonic acid-FITC diffusion was measured measured at the end of the protocol. (B) Size distribution (nm) and concentrations (particle/mL) of purified EVs from *P. freudenreichii* CIRM-BIA129 and (C) *P. freudenreichii* CIRM-BIA129ΔSlpB measured by nanoparticle tracking analysis. (D) Caco-2 cells grown on transwell for 21days were left untreated or pretreated with EVs from *P. freudenreichii* CIRM-BIA129 or *P. freudenreichii* CIRM-BIA129ΔSlpB (10^7 particles/well) for 24 hours on the apical side and then challenged or not with TNF-α and IFN-ɣ on the apical and basolateral side for 6 days, with a renewal at day 3. Sulfonic acid-FITC diffusion were measured at the end of the experiment. Data are expressed as means +/- SEM and normalized to control mean.

Figure 6. Deletion of SlpB surface protein exacerbates colitis. (A) Disease activity index (DAI) of the 3 groups (control, DSS and *P. freudenreichii* 129ΔSlpB+DSS) at day 11. (B) Paracellular and (C) transcellular permeabilities evaluated by measurement of sulfonic acid and HRP in animal plasma 4 hours after mice gavage. (D) Quantification of transcript levels

of *il-1β* (E) *tnf-α*, and (F) *il-10* measured at the end of the protocol in proximal colon of the four groups. Relative expression was determined using *Rps6* as reference. Values are expressed as means +/- SEM.

Supplemental Figure 1. *P. freudenreichii* CIRM-BIA129 mitigates DSS-induced colitis severity *in vivo*. Eight-week-old C57BL6 mice were gavaged during 11 days with milk ultra-filtrate (MUF) or MUF fermented by *P. freudenreichii* CIRM-BIA129(129) containing 1.10^8 CFU. At day 7, 4% DSS was added to drinking water or not. On day 11, permeabilities were measured, mice sacrificed and the tissues collected. (A) Bleeding score (B) stool consistency and (C) weight change before/after DSS of the 4 groups: control (MUF) or *P. freudenreichii* CIRM-BIA129 (129) in control conditions (grey) or with DSS (DSS and 129DSS in orange) at day 11.

REFERENCES

Alatab, Sudabeh, Sadaf G Sepanlou, Kevin Ikuta, Homayoon Vahedi, Catherine Bisignano, Saeid Safiri, Anahita Sadeghi, et al. 2020. 'The Global, Regional, and National Burden of Inflammatory Bowel Disease in 195 Countries and Territories, 1990–2017: A Systematic Analysis for the Global Burden of Disease Study 2017'. *The Lancet Gastroenterology & Hepatology* 5 (1): 17–30. https://doi.org/10.1016/S2468-1253(19)30333-4.

Arrieta, M C. 2006. 'Alterations in Intestinal Permeability'. *Gut* 55 (10): 1512–20. https://doi.org/10.1136/gut.2005.085373.

Belo, Giovanna A., Bárbara F. Cordeiro, Emiliano R. Oliveira, Marina P. Braga, Sara H. da Silva, Bruno G. Costa, Flaviano Dos S. Martins, et al. 2021. 'SlpB Protein Enhances the Probiotic Potential of *L. Lactis* NCDO 2118 in Colitis Mice Model'. *Frontiers in Pharmacology* 12: 755825. https://doi.org/10.3389/fphar.2021.755825.

Capurso, Lucio. 2019. 'Thirty Years of Lactobacillus Rhamnosus GG: A Review'. *Journal of Clinical Gastroenterology* 53 (Supplement 1): S1–41. https://doi.org/10.1097/MCG.0000000000001170.

Carmo, Fillipe L. R. do, Houem Rabah, Rodrigo D. De Oliveira Carvalho, Floriane Gaucher, Barbara F. Cordeiro, Sara H. da Silva, Yves Le Loir, Vasco Azevedo, and Gwénaël Jan. 2018. 'Extractable Bacterial Surface Proteins in Probiotic–Host Interaction'. *Frontiers in Microbiology* 9 (April): 645. https://doi.org/10.3389/fmicb.2018.00645.

Carmo, Fillipe L. R. do, Houem Rabah, Song Huang, Floriane Gaucher, Martine Deplanche, Stéphanie Dutertre, Julien Jardin, Yves Le Loir, Vasco Azevedo, and Gwénaël Jan. 2017. 'Propionibacterium Freudenreichii Surface Protein SlpB Is Involved in Adhesion to Intestinal HT-29 Cells'. *Frontiers in Microbiology* 8 (June): 1033. https://doi.org/10.3389/fmicb.2017.01033.

Carmo, Fillipe L. R. do, Wanderson M. Silva, Guilherme C. Tavares, Izabela C. Ibraim, Barbara F. Cordeiro, Emiliano R. Oliveira, Houem Rabah, et al. 2018. 'Mutation of the Surface Layer Protein SlpB Has Pleiotropic Effects in the Probiotic Propionibacterium Freudenreichii CIRM-BIA 129'. *Frontiers in Microbiology* 9 (August): 1807. https://doi.org/10.3389/fmicb.2018.01807.

Carmo, Fillipe Luiz Rosa do, Houem Rabah, Barbara Fernandes Cordeiro, Sara Heloisa da Silva, Rafaela Miranda Pessoa, Simone Odília Antunes Fernandes, Valbert Nascimento Cardoso, et al. 2019. 'Probiotic Propionibacterium Freudenreichii Requires SlpB Protein to Mitigate Mucositis Induced by Chemotherapy'. *Oncotarget* 10 (68): 7198–7219. https://doi.org/10.18632/oncotarget.27319.

Chang, Jeff, Rupert W. Leong, Valerie C. Wasinger, Matthew Ip, Michael Yang, and Tri Giang Phan. 2017. 'Impaired Intestinal Permeability Contributes to Ongoing Bowel Symptoms in Patients With Inflammatory Bowel Disease and Mucosal Healing'. *Gastroenterology* 153 (3): 723-731.e1. https://doi.org/10.1053/j.gastro.2017.05.056.

Cooper, H. S., S. N. Murthy, R. S. Shah, and D. J. Sedergran. 1993. 'Clinicopathologic Study of Dextran Sulfate Sodium Experimental Murine Colitis'. *Laboratory Investigation; a Journal of Technical Methods and Pathology* 69 (2): 238–49.

Coquenlorge, Sabrina, Laurianne Van Landeghem, Julie Jaulin, Nicolas Cenac, Nathalie Vergnolle, Emilie Duchalais, Michel Neunlist, and Malvyne Rolli-Derkinderen. 2016. 'The Arachidonic Acid Metabolite 11β-ProstaglandinF2α Controls Intestinal Epithelial Healing: Deficiency in Patients with Crohn's Disease'. *Scientific Reports* 6 (1): 25203. https://doi.org/10.1038/srep25203.

Deutsch, Stéphanie-Marie, Mahendra Mariadassou, Pierre Nicolas, Sandrine Parayre, Rozenn Le Guellec, Victoria Chuat, Vincent Peton, et al. 2017. 'Identification of Proteins Involved in the Anti-Inflammatory Properties of *Propionibacterium Freudenreichii* by Means of a Multi-Strain Study'. *Scientific Reports* 7 (April): 46409. https://doi.org/10.1038/srep46409.

Foligné, B., J. Breton, D. Mater, and G. Jan. 2013. 'Tracking the Microbiome Functionality: Focus on *Propionibacterium* Species'. *Gut* 62 (February): 1227–28.

Foligné, B., S. M. Deutsch, J. Breton, F. J. Cousin, J. Dewulf, M. Samson, B. Pot, and G. Jan. 2010. 'Promising Immunomodulatory Effects of Selected Strains of Dairy Propionibacteria as Evidenced *in Vitro* and *in Vivo*'. *Applied and Environmental Microbiology* 76 (December): 8259–64.

Foligné, Benoît, Stéphanie-Marie Deutsch, Jérôme Breton, Fabien J. Cousin, Joëlle Dewulf, Michel Samson, Bruno Pot, and Gwénaël Jan. 2010. 'Promising Immunomodulatory Effects of Selected Strains of Dairy Propionibacteria as Evidenced *In Vitro* and *In Vivo*'. *Applied and Environmental Microbiology* 76 (24): 8259–64. https://doi.org/10.1128/AEM.01976-10.

Illikoud, Nassima, Marine Mantel, Malvyne Rolli-Derkinderen, Valérie Gagnaire, and Gwénaël Jan. 2022. 'Dairy Starters and Fermented Dairy Products Modulate Gut Mucosal Immunity'. *Immunology Letters* 251–252 (December): 91–102. https://doi.org/10.1016/j.imlet.2022.11.002.

Konstantinov, Sergey R., Hauke Smidt, Willem M. De Vos, Sven C. M. Bruijns, Satwinder Kaur Singh, Florence Valence, Daniel Molle, et al. 2008. 'S Layer Protein A of *Lactobacillus Acidophilus* NCFM Regulates Immature Dendritic Cell and T Cell Functions'. *Proceedings of*

the National Academy of Sciences 105 (49): 19474–79. https://doi.org/10.1073/pnas.0810305105.

Lê, Amélie, Marine Mantel, Justine Marchix, Marie Bodinier, Gwénaël Jan, and Malvyne Rolli-Derkinderen. 2022. 'Inflammatory Bowel Disease Therapeutic Strategies by Modulation of the Microbiota: How and When to Introduce Pre-, pro-, Syn-, or Postbiotics?' *American Journal of Physiology. Gastrointestinal and Liver Physiology* 323 (6): G523–53. https://doi.org/10.1152/ajpgi.00002.2022.

Le Berre, Catherine, Philippe Naveilhan, and Malvyne Rolli-Derkinderen. 2023. 'Enteric Glia at Center Stage of Inflammatory Bowel Disease'. *Neuroscience Letters* 809 (July): 137315. https://doi.org/10.1016/j.neulet.2023.137315.

Le Marechal, C., V. Peton, C. Ple, C. Vroland, J. Jardin, V. Briard-Bion, G. Durant, et al. 2015. 'Surface Proteins of *Propionibacterium Freudenreichii* Are Involved in Its Anti-Inflammatory Properties'. *J.Proteomics.* 113C (January): 447–61.

Le Maréchal, Caroline, Vincent Peton, Coline Plé, Christophe Vroland, Julien Jardin, Valérie Briard-Bion, Gaël Durant, et al. 2015. 'Surface Proteins of Propionibacterium Freudenreichii Are Involved in Its Anti-Inflammatory Properties'. *Journal of Proteomics* 113 (January): 447–61. https://doi.org/10.1016/j.jprot.2014.07.018.

Lebeer, Sarah, Jos Vanderleyden, and Sigrid C. J. De Keersmaecker. 2010. 'Host Interactions of Probiotic Bacterial Surface Molecules: Comparison with Commensals and Pathogens'. *Nature Reviews Microbiology* 8 (3): 171–84. https://doi.org/10.1038/nrmicro2297.

Lightfoot, Yaíma L, Kurt Selle, Tao Yang, Yong Jun Goh, Bikash Sahay, Mojgan Zadeh, Jennifer L Owen, et al. 2015. 'SIGNR 3-dependent Immune Regulation by *Lactobacillus Acidophilus* Surface Layer Protein A in Colitis'. *The EMBO Journal* 34 (7): 881–95. https://doi.org/10.15252/embj.201490296.

Ma, Seongho, Jiah Yeom, and Young-Hee Lim. 2020. 'Dairy Propionibacterium Freudenreichii Ameliorates Acute Colitis by Stimulating MUC2 Expression in Intestinal Goblet Cell in a DSS-Induced Colitis Rat Model'. *Scientific Reports* 10 (1): 5523. https://doi.org/10.1038/s41598-020-62497-8.

Malik, A. C., G. W. Reinbold, and E. R. Vedamuthu. 1968. 'An Evaluation of the Taxonomy of *Propionibacterium*'. *Canadian Journal of Microbiology* 14 (11): 1185–91. https://doi.org/10.1139/m68-199.

Mantel, Marine, Tales Fernando Da Silva, Rafael Gloria, Danièle Vassaux, Kátia Duarte Vital, Valbert Nascimento Cardoso, Simone Odília Antunes Fernandes, et al. 2023. 'Fat Matters: Fermented Whole Milk Potentiates the Anti-Colitis Effect of Propionibacterium Freudenreichii'. *Journal of Functional Foods* 106 (July): 105614. https://doi.org/10.1016/j.jff.2023.105614.

Munkholm, P, E Langholz, D Hollander, K Thornberg, M Orholm, K D Katz, and V Binder.

1994. ‘Intestinal Permeability in Patients with Crohn’s Disease and Ulcerative Colitis and Their First Degree Relatives.’ *Gut* 35 (1): 68–72. https://doi.org/10.1136/gut.35.1.68.

Pearson, A D, E J Eastham, M F Laker, A W Craft, and R Nelson. 1982. ‘Intestinal Permeability in Children with Crohn’s Disease and Coeliac Disease.’ *BMJ* 285 (6334): 20–21. https://doi.org/10.1136/bmj.285.6334.20.

Peeters, Marc, Yvo Ghoos, Bart Maes, Martin Hiele, Karel Geboes, Gaston Vantrappen, and Paul Rutgeerts. 1994. ‘Increased Permeability of Macroscopically Normal Small Bowel in Crohn’s Disease’. *Digestive Diseases and Sciences* 39 (10): 2170–76. https://doi.org/10.1007/BF02090367.

Pochard, Camille, Sabrina Coquenlorge, Julie Jaulin, Nicolas Cenac, Nathalie Vergnolle, Guillaume Meurette, Marie Freyssinet, Michel Neunlist, and Malvyne Rolli-Derkinderen. 2016. ‘Defects in 15-HETE Production and Control of Epithelial Permeability by Human Enteric Glial Cells From Patients With Crohn’s Disease’. *Gastroenterology* 150 (1): 168–80. https://doi.org/10.1053/j.gastro.2015.09.038.

Pochard, Camille, Jacques Gonzales, Anne Bessard, Maxime M. Mahe, Arnaud Bourreille, Nicolas Cenac, Anne Jarry, et al. 2021. ‘PGI2 Inhibits Intestinal Epithelial Permeability and Apoptosis to Alleviate Colitis’. *Cellular and Molecular Gastroenterology and Hepatology* 12 (3): 1037–60. https://doi.org/10.1016/j.jcmgh.2021.05.001.

Prigent, Alice, Guillaume Chapelet, Adrien De Guilhem De Lataillade, Thibauld Oullier, Emilie Durieu, Arnaud Bourreille, Emilie Duchalais, et al. 2020. ‘Tau Accumulates in Crohn’s Disease Gut’. *The FASEB Journal* 34 (7): 9285–96. https://doi.org/10.1096/fj.202000414R.

Prigent, Alice, Arthur Lionnet, Emilie Durieu, Guillaume Chapelet, Arnaud Bourreille, Michel Neunlist, Malvyne Rolli-Derkinderen, and Pascal Derkinderen. 2019. ‘Enteric Alpha-Synuclein Expression Is Increased in Crohn’s Disease’. *Acta Neuropathologica* 137 (2): 359–61. https://doi.org/10.1007/s00401-018-1943-7.

Rabah, Houem, Olivia Ménard, Floriane Gaucher, Fillipe Luiz Rosa do Carmo, Didier Dupont, and Gwénaël Jan. 2018a. ‘Cheese Matrix Protects the Immunomodulatory Surface Protein SlpB of Propionibacterium Freudenreichii during in Vitro Digestion’. *Food Research International* 106 (April): 712–21. https://doi.org/10.1016/j.foodres.2018.01.035.

———. 2018b. ‘Cheese Matrix Protects the Immunomodulatory Surface Protein SlpB of *Propionibacterium Freudenreichii* during in Vitro Digestion’. *Food Res. Int.* 106 (April): 712–21. https://doi.org/10.1016/j.foodres.2018.01.035.

Rodovalho, Vinícius de Rezende, Brenda Silva Rosa da Luz, Houem Rabah, Fillipe Luiz Rosa do Carmo, Edson Luiz Folador, Aurélie Nicolas, Julien Jardin, et al. 2020. ‘Extracellular Vesicles Produced by the Probiotic Propionibacterium Freudenreichii CIRM-BIA 129 Mitigate Inflammation by Modulating the NF-κB Pathway’. *Frontiers in Microbiology* 11 (July): 1544. https://doi.org/10.3389/fmicb.2020.01544.

Sniffen, Jason C., Lynne V. McFarland, Charlesnika T. Evans, and Ellie J. C. Goldstein. 2018. 'Choosing an Appropriate Probiotic Product for Your Patient: An Evidence-Based Practical Guide'. Edited by Leandro Araujo Lobo. *PLOS ONE* 13 (12): e0209205. https://doi.org/10.1371/journal.pone.0209205.

Suzuki, Asuka, Keiichi Mitsuyama, Hironori Koga, Nobuo Tomiyasu, Junya Masuda, Kosuke Takaki, Osamu Tsuruta, Atsushi Toyonaga, and Michio Sata. 2006. 'Bifidogenic Growth Stimulator for the Treatment of Active Ulcerative Colitis: A Pilot Study'. *Nutrition* 22 (1): 76–81. https://doi.org/10.1016/j.nut.2005.04.013.

Tindemans, Irma, Maria E. Joosse, and Janneke N. Samsom. 2020. 'Dissecting the Heterogeneity in T-Cell Mediated Inflammation in IBD'. *Cells* 9 (1): 110. https://doi.org/10.3390/cells9010110.

Turner, Jerrold R. 2009. 'Intestinal Mucosal Barrier Function in Health and Disease'. *Nature Reviews Immunology* 9 (11): 799–809. https://doi.org/10.1038/nri2653.

Wang, Jing, Haifeng Ji, Sixin Wang, Hui Liu, Wei Zhang, Dongyan Zhang, and Yamin Wang. 2018. 'Probiotic Lactobacillus Plantarum Promotes Intestinal Barrier Function by Strengthening the Epithelium and Modulating Gut Microbiota'. *Frontiers in Microbiology* 9 (August): 1953. https://doi.org/10.3389/fmicb.2018.01953.

Wyatt, J., H. Vogelsang, W. Hübl, T. Waldhoer, and H. Lochs. 1993. 'Intestinal Permeability and the Prediction of Relapse in Crohn's Disease'. *The Lancet* 341 (8858): 1437–39. https://doi.org/10.1016/0140-6736(93)90882-H.

Yan, Fang, and D. Brent Polk. 2012. 'Characterization of a Probiotic-Derived Soluble Protein Which Reveals a Mechanism of Preventive and Treatment Effects of Probiotics on Intestinal Inflammatory Diseases'. *Gut Microbes* 3 (1): 25–28. https://doi.org/10.4161/gmic.19245.

Table 1. Disease Activity Index.

Score	Weight loss (%)	Stool consistency	Occult/Gross bleeding
0	<1%	Normal	Negative
1	1-5%		Stain
2	5-10%	Loose	Occult blood
3	10-15%		
4	>15%	Diarrhea	Gross bleeding

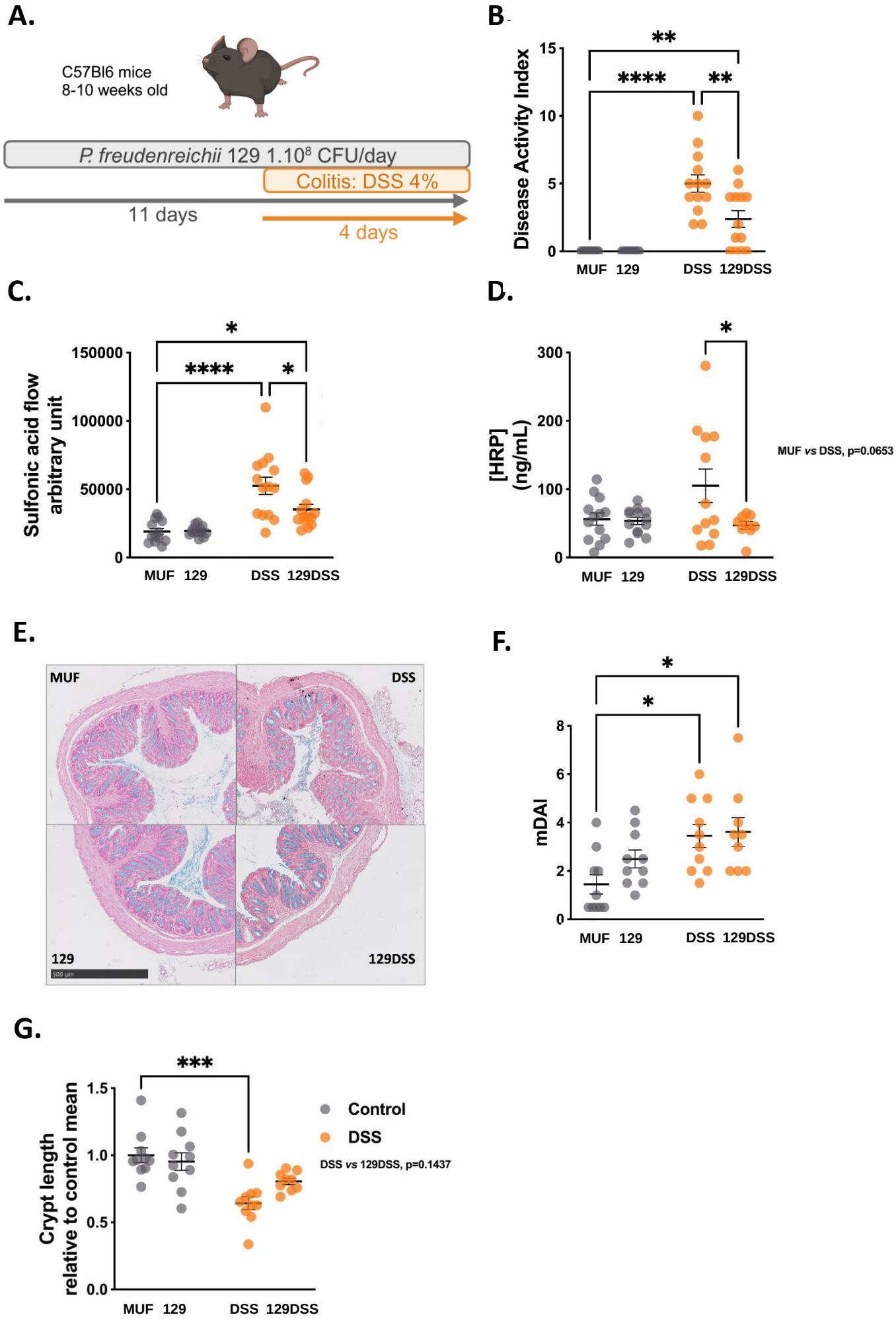

Figure 1

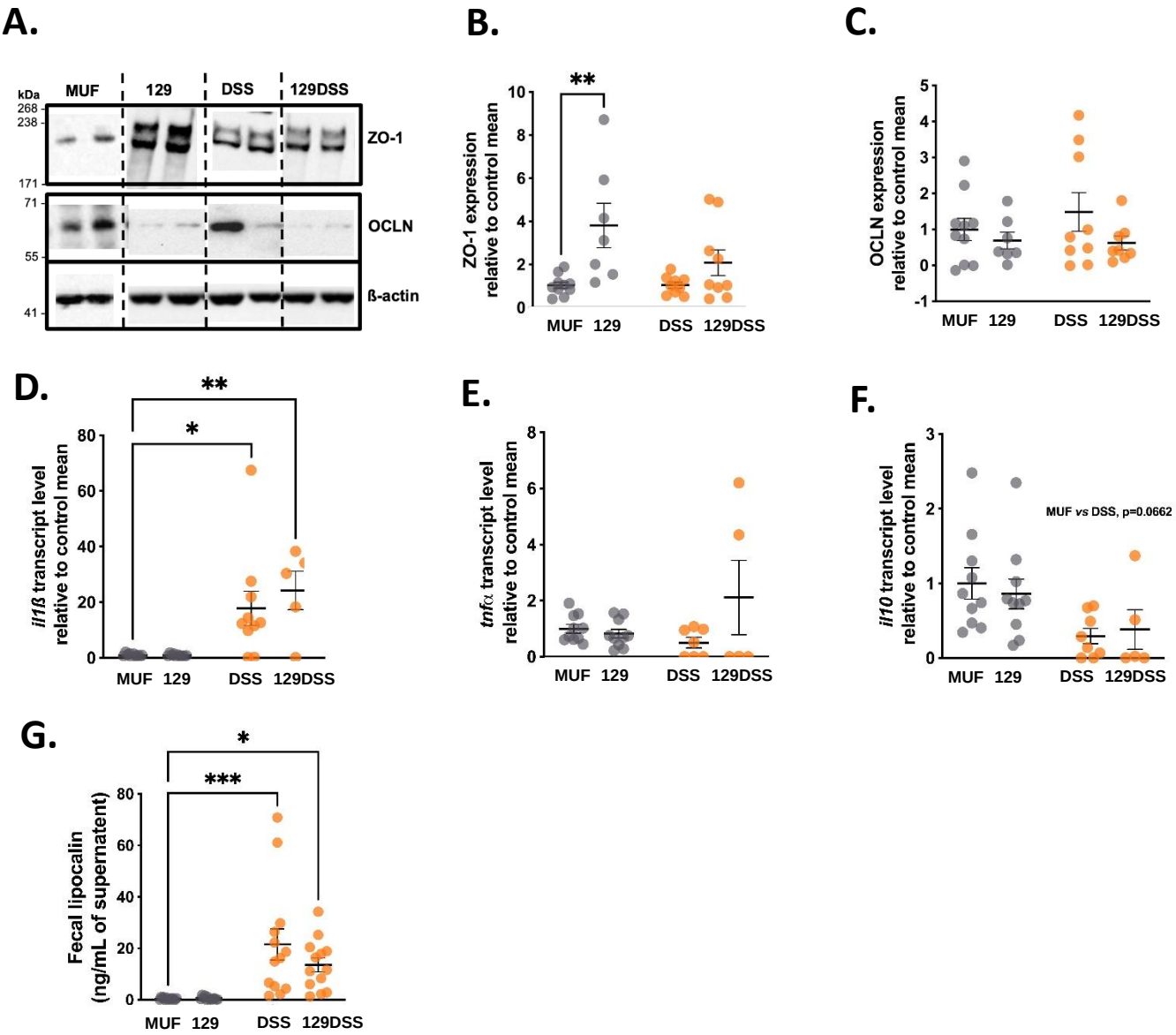

Figure 2

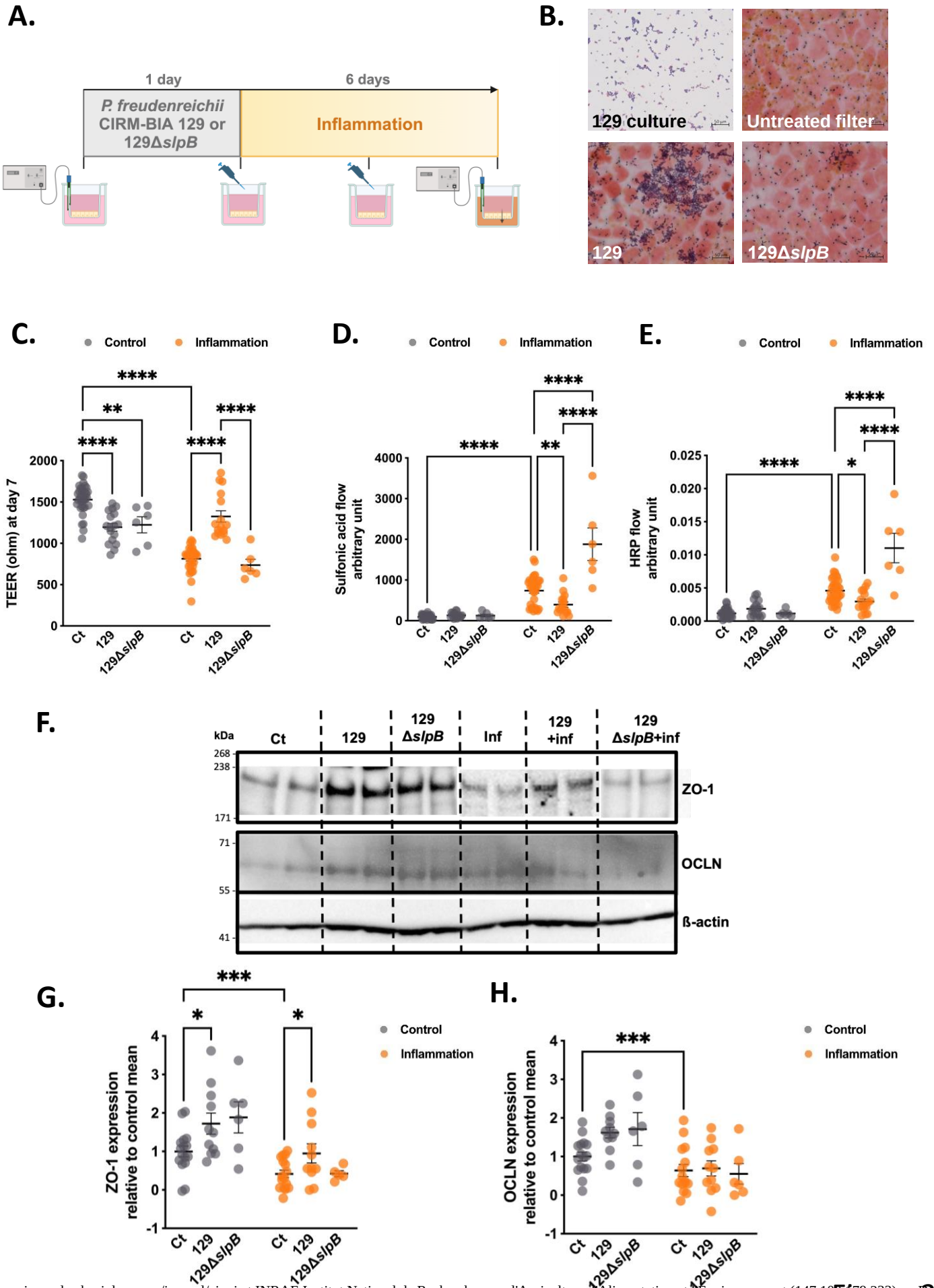

Figure 3

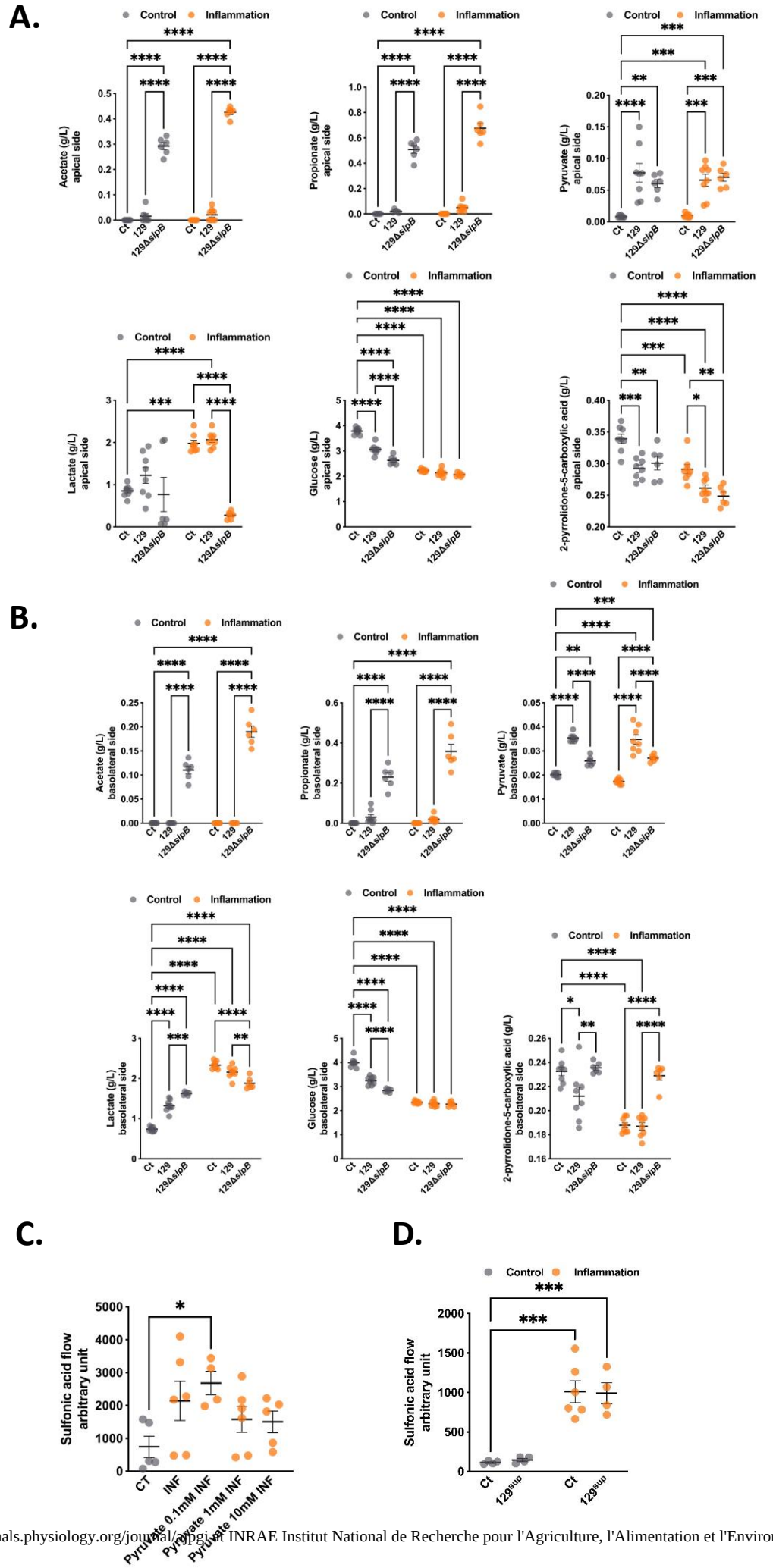

Figure 4

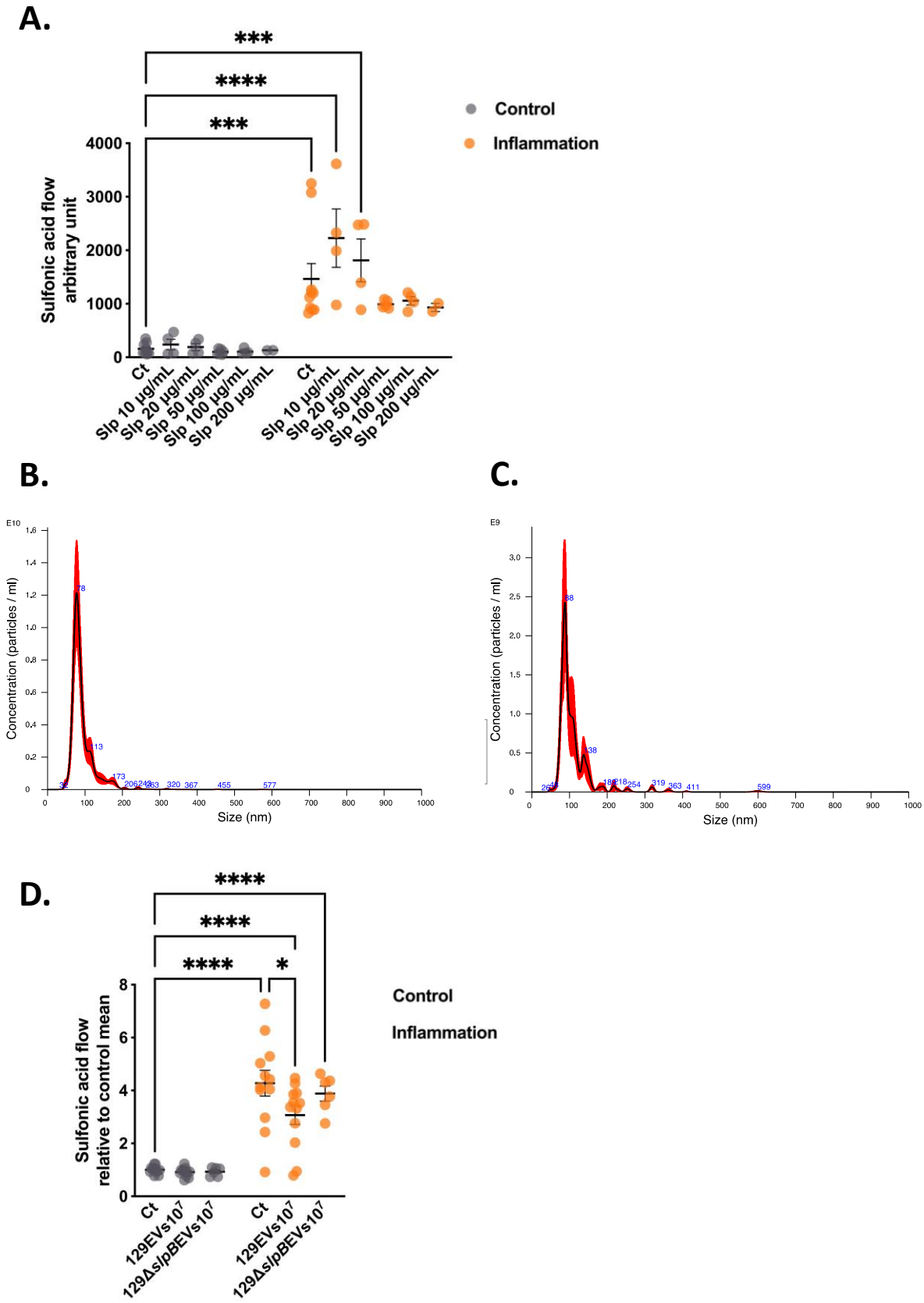

Figure 5

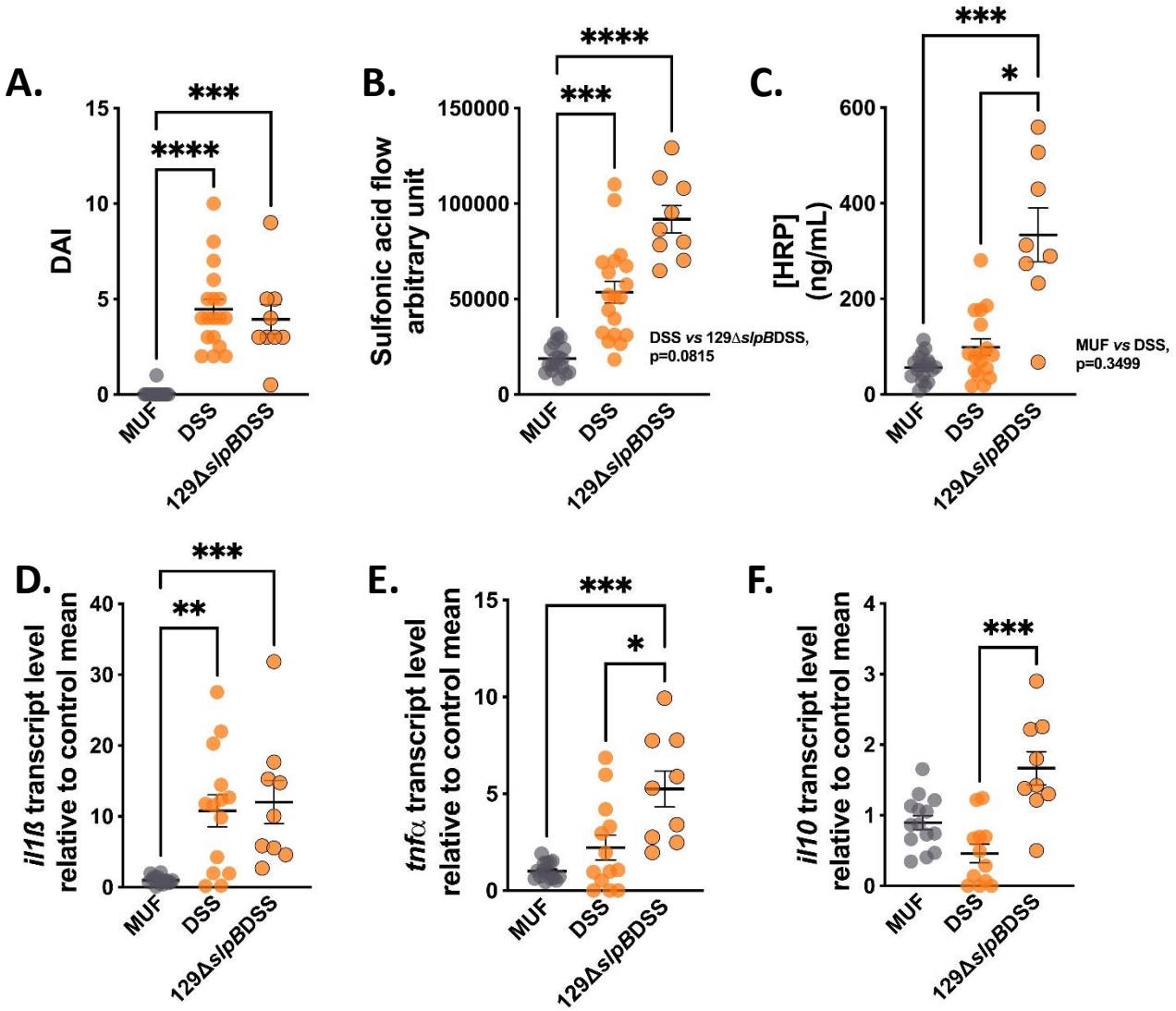

Figure 6

Graphical Abstract